Effect of nitrogen concentration on microstructure and microhardness of nanostructured (Ti, Al, Si)N coatings developed by d.c. reactive magnetron sputtering

D. BIRO, L. JAKAB-FARKAS, G. STRNAD[*a], V. BOLOS[a], I. VIDA-SIMITI[b]
Sapientia University, Faculty of Engineering, 540485 Tg. Mures, Romania
[a] *Petru Maior University, Faculty of Engineering, 540088 Tg. Mures, Romania*
[b]*Technical University, Faculty of Materials Science and Engineering, 400641 Cluj-Napoca, Romania*

Nanostructured (Ti, Al, Si)N thin film coatings were synthesized by d.c. reactive magnetron sputtering, performed in an Ar/N_2 gas mixture from a planar rectangular Al:Ti:Si=50:25:25 alloyed target. The mass flow of N_2 reactive gas was strictly controlled in sputtering process. Cross-sectional transmission electron microscopy (XTEM) investigation performed through the deposited films revealed distinct microstructure evolution for different samples. It was found that the variation of the reactive gas amount induced changes in film microstructure. The metallic AlTiSi coating, developed in the absence of the reactive gas, exhibited strong columnar growth with a polycrystalline structure. The addition of a small amount of nitrogen to the process gas leads to a crystallite refinement. Further increase in nitrogen amount leads to a nanocomposite structure consisting of crystalline Ti_3AlN nanograins in 2…3 nm size surrounded by an amorphous Si_xN_y and/or AlN matrix phase The microhardness of as-deposited (Ti, Al, Si)N coatings was measured using a CV-400 AAT microhardness tester and was found in 4...24 GPa range.

1. Introduction

Nanocomposite coating materials, consisting of a nanocrystalline transition metal nitride and an amorphous tissue phase, gained recently a special interest due to their unusual mechanical properties. These coating materials are characterized by high hardness [1], enhanced elasticity [2] and high thermal stability [3]. Some study revealed that the ratio between hardness and elastic modulus H/E plays an important role to the coating performance. Furthermore, some study also emphasized that in multiphase nanocomposite materials the microstructure plays an important role [4].

As was suggested by Veprek [5], in nanocomposite materials the structure and size of nanocrystalline grains embedded in the amorphous tissue phase as well as the high cohesive energy at their interfaces, are the main parameters which are influencing the mechanical behaviour of the coatings. The reported results revealed that adatom mobility may control the microstructure evolution in multielemental coating systems, where the substrate temperature and the low energy ion/atom arrival rate have significant effect on growth of nanocrystalline grains.

In the last decade intense research activity was devoted to provide techniques and design architecture of process parameters for deposition of multiphase nanocomposite materials. The reactive d.c. and r.f. magnetron sputtering, arc plasma PVD techniques are the main established technologies used in plasma assisted deposition of thin films coating. The most studied material is the quaternary (Ti, Al, Si)N nitride system which revealed the most promising results.

Microstructure and growth mechanism of arc plasma deposited TiAlSiN (35 at.% Ti, 42 at.% Al, 6.5 at.% Si) thin films were investigated using conventional and high-resolution transmission electron microscopy by Parlinska at al. [6, 7]. The Ti-rich zone of coating close to the substrate exhibited crystalline structure with pronounced columnar growth. The addition of Al+Si leads to a crystallite refinement of the coatings, and a further increasing of the Al+Si concentration resulted in the formation of nanocomposites, consisting of equiaxial, crystalline nanograins surrounded by a disordered, amorphous Si_xN_y matrix.

Regarding the microhardness of nanocomposite coatings Veprek, in his well known review paper "Different approaches to superhard coatings and nanocomposites" [8] showed that there are two mechanisms that leads to the increase of hardness in hard and superhard coatings. One is hardness enhancement by energetic ion bombardment. This phenomenon is due to a complex, synergistic effect involving a decrease of crystallite size, densification of the grain boundaries, formation of Frenkel pairs and other point defects, and built-in biaxial compressive stress. The second is the mechanism of hardness enhancement by the formation of a stable nanocomposite structure due to self-organization upon spinodal phase segregation. This concept is based on a strong, thermodynamically driven, and diffusion rate-controlled (spinodal) phase segregation that leads to the formation of a stable nanostructure by self-organization. In

the case of superhard, thermally highly stable nanocomposites the dislocation activity is absent. These materials consist of a few-nanometer small crystallites of a hard transition metal nitride (or carbide, boride) "glued" together by about one-monolayer-thin layer of nonmetallic, covalent nitride such as Si_3N_4, BN (or in the case of carbides by excess carbon, CN_x, and others). Depending on the crystallite size in the given material, the effects mentioned above may hinder the dislocation activity. These coatings, when correctly prepared, posses an unusual combination of mechanical properties, such as a high hardness of 40 to 100 GPa, high elastic recovery of 80% to 94%, elastic strain limit of >10%, and high tensile strength of 10 to ≥40 GPa.

In nc-TiN/a-Si_3N_4 spinodal phase segregation is thermodynamically driven by a high activity (partial pressure) of nitrogen, and rate-controlled by diffusion that requires a sufficiently high temperature. A sufficiently high activity of nitrogen (partial pressure of >10^{-5} bar) is needed in order to provide the necessary thermodynamic driving force for spinodal decomposition to occur during deposition that results in the formation of an nc-TiN/a-Si_3N_4 nanocomposite with a small and regular crystallite size. The hardness reaches a maximum of 50–60 GPa at a silicon content of about 8–10 at.% when the nanocrystals of the transition metal nitrides are covered with about one monolayer of silicon nitride [8].

Prochazka showed that the maximum achievable hardness in nc-TiN/a-Si_3N_4 nanocomposites deposited by reactive magnetron sputtering under a sufficiently high nitrogen pressure of ≥0.001 mbar (a higher pressure is desirable, but its use limits the deposition rate) and deposition temperature of 550–650˚C is controlled by the oxygen impurity concentration [9]. Regarding the microstructure, coatings deposited by PVD at relatively low temperatures of 300–600˚C have a columnar morphology whose development is described by the Thornton structure zone diagram. When superhard nanocomposites with the optimum composition are formed, this columnar structure vanishes. The development of an isotropic and dense nanostructure upon the formation of stable superhard nanocomposites is an important result because the columnar morphology, even if within the dense T-zone, still suffers in terms of mechanical properties due to weaker bonding between the columns. Therefore, the complete vanishing of the columnar morphology in the nanocomposites deposited by PVD is important to the excellent mechanical properties of these nanocomposites. Veprek, citing the work of Karvankova et al. [9], showed that although the morphology of the nanocomposites with the highest hardness deposited by magnetron sputtering appears isotropic, a more detailed investigation by TEM reveals that there is still a sign of a slightly columnar, quite dense morphology [8].

In this paper (Ti, Al, Si)N single layered thin film coatings deposited on mono-crystalline Si (100) and polycrystalline high-speed steel substrates produced by d.c. reactive magnetron sputtering were studied. The objective of this study is to investigate microstructural changes and microhardness of coatings in (Ti, Al, Si)N thin films as a function of nitrogen concentration.

2. Experimental details

Deposition experiments of (Ti, Al, Si)N quaternary nitride coatings were carried out in a laboratory scale equipment by d.c. driven magnetron sputtering, whose details are reported elsewhere [10]. The three independent sputter sources were closely arranged side by side on the neighbouring vertical walls of a 75 l octagonal all-metal high vacuum chamber. The closely disposed UM magnetrons arranged on an arc segment were highly interacting by their magnetic fields, leading to a far extended active plasma volume. In the present deposition experiments only the central magnetron source was active, while the adjacent two magnetron sources contributed only in generating of closed magnetic field (Fig. 1). A high purity planar rectangular target material of alloyed AlTiSi was used. Elemental composition of the alloyed target was 50 at.% Al, 25 at.% Ti and 25 at.% Si, with 165x85x12 mm^3 in size, which was partially covered on the erosion zone with a Ti sheet. Prior to deposition a base pressure of $2 \cdot 10^{-4}$ Pa was established by operating a 540 l/s turbomolecular pump.
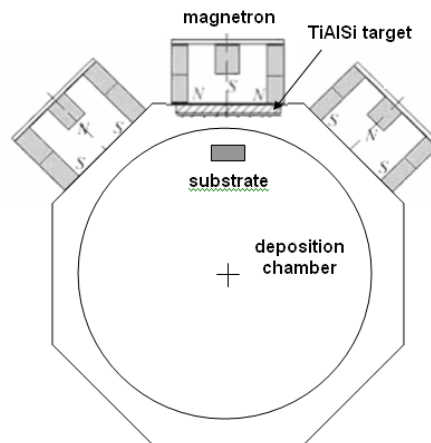

Fig 1. Schematic illustration of the experimental setup

The substrates were high-speed steel (HSS) for microhardness measurements, and <100> Si wafers covered by thermally grown SiO_2 for structure characterization. The target-to-substrate distance was kept constant at 110 mm in all runs. The substrates were positioned in static mode on a molybdenum sheet substrate holder, which allowed application of $U_s = -75$ V bias voltage. The Mo sheet was externally heated for a controllable substrate temperature of $T_s = 400$ ºC. Prior to the starting of the deposition process the surface of substrates were plasma-etched by a d.c. glow discharge in argon for 10 min at 0.8 Pa, while the bias voltage has been limited up to 350 V. During the ion etching of substrates, the target surfaces were also sputter cleaned by operating the magnetron unit at limited discharge power (pre-sputtering power 150 W). The substrate surfaces were

shielded during the pre-sputtering. After about 10 min sputter cleaning of the targets, the discharge power at the target was raised to 500 W and the development of coating started with the deposition of a 50 nm thick AlTiSi seed-layer in pure Ar atmosphere. In the next step a gradient (Ti, Al, Si)(N) interlayer were reactively deposited with the same sputtering power of the target, while N_2 flow rate was increased slowly up to the designed value. The argon gas flow was kept constant at 6.0 sccm. The typical thickness of the coatings was approximately 2 µm.

The reactive sputtering process was performed in a mixture of Ar and N_2 atmosphere at 0.18 Pa. During of the reactive sputtering process the nitrogen mass flow rate was controlled with an Aalborg DFC 26, which contains a solenoid valve. The argon gas throughput (q_{Ar}=6.0 sccm, measured by GFM 17 Aalborg mass flow meter) was adjusted by a servomotor driven mass flow rate controller (MFC-Granville Phillips S 216). A constant sputtering power of 500 W, with a current density rough of 10 mA/cm^2 in the target, was selected during of deposition. The experimental conditions for preparation of (Ti, Al, Si)N coatings are listed in Table 1.

Table 1. Summary of deposition parameters used for preparation of (Ti, Al, Si)N coatings

Sample	Magnetron power $P_{Ti-Al-Si}$ [W]	Gas flow q_{N2} [sccm]	Substrate temperature T_s [°C]	Bias voltage U_s [V]
TiS-01	500	-	400	-75
TiS-07	500	1.0	400	-75
TiS-08	500	1.0	400	-75
TiS-04	500	2.0	400	-75
TiS-09	500	2.0	400	-75
TiS-10	500	2.0	100	-75
TiS-06	500	3.0	400	-75
TiS-03	500	4.0	400	-75
TiS-05	500	5.0	400	-75
TiS-02	500	6.0	400	-75

The microstructure of the as-deposited coatings, such as size and morphology of the crystals were examined by a 100 kV voltage operated JEOL 100U transmission electron microscope. To prepare cross-sectional XTEM samples for transverse observations, the samples were subjected to ion-milling in view of thinning up to electron beam transparency. Thin specimens for XTEM investigations were prepared in Technoorg-Linda IV/H/L ion beam thinning unit. High energy ion beam thinning was completed with a low angle and low energy (200 eV) ion beam process in order to eliminate the amorphous by-products and etching defects induced by the high energy ions. Bright-field (BF) and dark-field (DF) imaging techniques were used for microstructure investigation of the as-prepared samples. The identification of the crystallographic phases and the crystal orientation was performed also by investigation of selected area electron diffraction (SAED) patterns. The SAED patterns were processed and evaluated with the Process-Diffraction software tool developed by Labar [11].

Vickers microhardness was measured using a CV-400 AAT microhardness tester, with a load of 25 gf and 10 s for holding time.

3. Results and discussion

Transmission electron microscopy in conventional (TEM) mode has been used on samples that were thinned by the ion beam milling cross-section technique. In this XTEM study, performed to investigate the microstructure of our prepared (Ti, Al, Si)N nanocomposite coatings, we combined direct imaging and selected area electron diffraction modes (SAED), which facilitates to obtain information about the microstructure morphology, grain size and crystallographic preferred orientation. A typical example of the microstructure of TiAlSi coating is given in Fig. 2. The micrograph indicates cross sectional image of the crystalline coating. The crystallite in a conical evolution starts close to the substrate and are growing in a competitive mode up to approximately 80 nm in width throughout the film thickness.
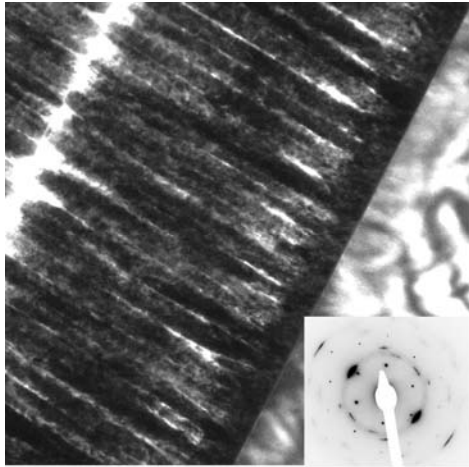
Fig. 2. XTEM micrograph showing a cross sectional view of the columnar structured polycrystalline AlTiSi thin film coating of sample TiS-01. The inset of SAED electron diffraction pattern indicates an fcc-structured TiAlSi solid solution phase, showing (200) texture evolution in the growing direction.

The elongated crystallites are growing through the entire film thickness up to the top surface of the coating. The columnar crystallites are normally oriented to the substrate's surface. Large crystallites in size of approximately 80 nm are separated by the more electron transparent $TiSi_2$ phase segregated to the grain boundaries. The SAED patterns taken from the bulk region of the film (not shown here) exhibit well defined spotted diffraction rings. The SAED pattern taken from the near substrate region of the coating proved crystalline character of the Si doped TiAl film (inset of Fig. 2). The phases that can be derived from the diffraction pattern are mainly fcc-B1 NaCl type of TiAlSi solid solution and $TiSi_2$ crystallites. The simulation of the diffraction rings was performed taking into account an fcc-type structure. Clearly can be seen the <200> preferential growth direction, indicated by significant brightness increase due to reflections from (200) crystallite planes that are parallel oriented to the growing surface. The composition of the thin film was calculated from EDS spectra, and found to be: Ti: 34 at%, Al: 46 at% and Si: 20 at%.

By adding a small amount of nitrogen as reactive gas in argon process gas, the morphology of the film dramatically changed. For a nitrogen flow rate of $q_{N2} = 2$ sccm the microstructure indicate a weak columnar evolution (Fig. 3.a). Inside of the columns a development tendency of a slightly curved fine lamellae growth morphology could be identified (Fig. 3.b). The composition of the thin film was calculated from EDS spectra, and found to be: Ti: 23 at%, Al: 46 at% and Si: 30 at%. Nitrogen was not detected by this method in the film.

The selected area electron diffraction pattern revealed a grain refinement due to phase segregation and the consequent formation of polycrystalline grains in mixture with amorphous matrix phase (inset of Fig. 3.b).

The SAED pattern claims for two-phase mixture of TiAlN nanocrystals embedded in an amorphous silicon nitride tissue phase, while the (200) preferential growth is slightly maintained.
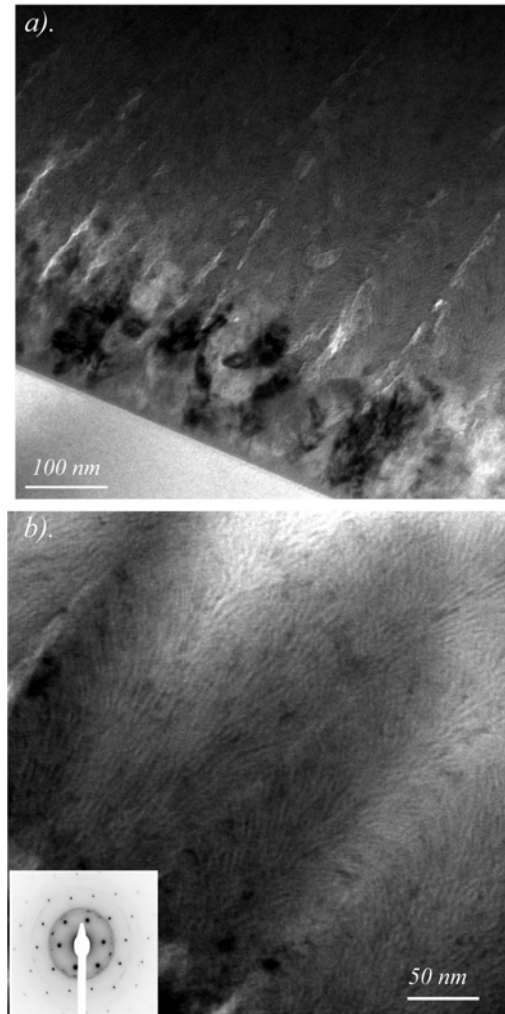

Fig. 3. XTEM micrograph images of coating (sample TiS-09) grown by nitrogen flow rate of $q_{N2} = 2$ sccm; a) Bright field (BF) image indicate a weakly columnar structure evolution in close to the interface; b) Enlarged image indicates transition from the ternary TiAlSi sub-layer to the quaternary (AlTiSi)N overgrown layer: the microstructure inside of the column's bulk shows a tendency for evolution in a curved fine lamellae morphology.

With further increase of the nitrogen amount in the film disappear the crystalline character of the coating and continue to develop a nanocomposite structure, possibly consisting of nanocrystalline $Ti_3AlN/TiSi_2$ grains of 2…3 nm in size surrounded by an amorphous Si_xN_y and/or AlN matrix phase (Fig. 4.a).

Selected area electron diffraction pattern revealed that an increased nitrogen amount leads to a nanocomposite structure, possibly consisting of equiaxial nanocrystalline $Ti_3AlN/TiSi_2$ grains surrounded by an amorphous Si_xN_y

and/or AlN matrix phase (Fig. 5). The composition of the thin film in TiS-05 sample was calculated from EDS spectra, and found to be: Ti: 12 at%, Al: 19 at%, Si: 23 at% and N: 46 at%.

Based on X-ray diffraction (XRD) data investigation reported by Carvalho et. al. [12, 13] an increase in the lattice parameter from 0.418 nm to 0.429 nm of the (Ti, Al, Si)N nanocomposite coating has been reported, when the adatom mobility was changed. The lowest lattice parameter corresponded to a Ti-Al-Si-N phase where some of the Si and Al atoms are occupying Ti positions in the fcc-TiN lattice. The highest lattice parameter was associated to a system where a partial Si segregation occurred, which might be enough to nucleate and develop a Si_3N_4 phase. It has been suggested that Si_3N_4 tissue phase forms a covering layer on the growth surface of the (Ti, Al)N nanocrystallites, limiting their growth.

Fig. 5. SAED diffraction pattern of randomly oriented nanocrystalline $Ti_3AlN/TiSi_2$ grains surrounded by an amorphous Si_xN_y and/or AlN matrix phase.
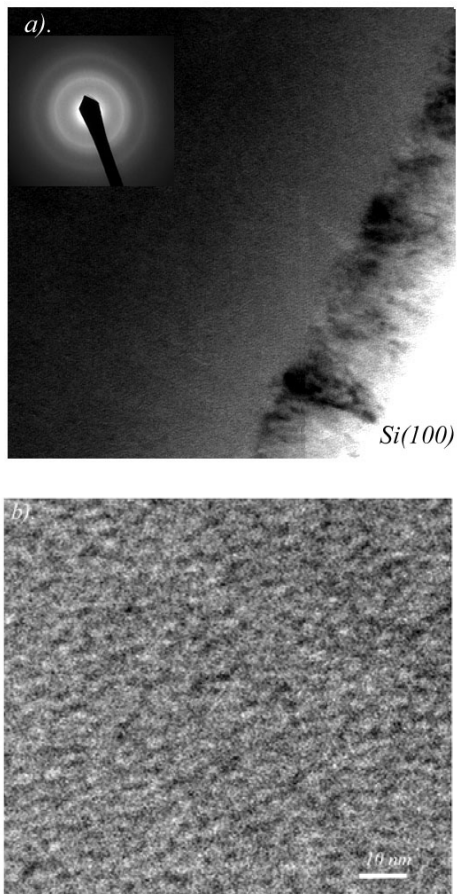

Fig. 4. Bright field XTEM images and SAED diffraction pattern of (AlTiSi)N thin film coating (TiS-05 sample, q_{N2} = 5 sccm): a) The microstructure near the film-substrate interface indicate a competitive columnar evolution in close to the interface of the (AlTiSi)N thin film coating and a nanograin structure with disordered grain limiting boundaries; b) The enlarged micrograph clearly shows randomly distribution of the very fine grains, having the average size of ~ 3 nm.
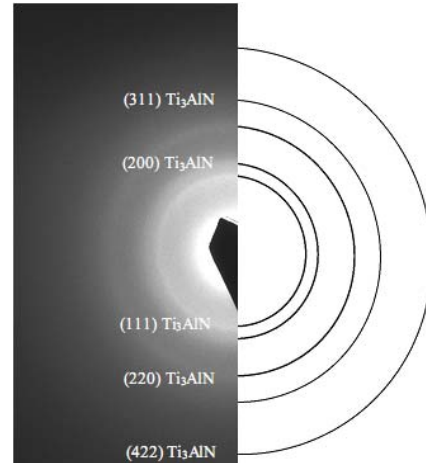
Formation of AlN precipitation due to the partial segregation of Al atoms, it should be considered also due to the effect of enhanced ion bombardment provided by the focused plasma beam, that is characteristic for the present experimental conditions [10]. When atomic surface mobility in the growing film is adequate, due to the high deposition temperature and/or due to an energy transfer from an increased incident ion-to-atom arrival rate ratio, the segregated atoms can nucleate and develop the new phase [14]. The increase in deposition rate induces a decrease in the surface mobility related with the decrease of the ion-to-atom arrival rate ratio. These particular deposition conditions explain the columnar structure of sample, which is clearly seen in the dark field image. From the detailed observation of the SAED diffuse diffraction pattern, the presence of an amorphous phase surrounding the Ti_3AlN nanocrystallites can be attributed to Si_xN_y matrix. Addition of minor amounts of Si_xN_y leads to an encapsulation of the growing TiAlN crystallites and hindering their growth. The grain size of the coating material decreases with increasing concentration of amorphous tissue phase material.

Table 2 presents the results of Vickers microhardness test applied on selected coatings deposited on HSS substrates. In Fig. 6 the values of microhardness are plotted vs. N_2/Ar gases flow rates (the argon gas flow was kept constant at 6.0 sccm).

Table 2. Results of Vickers microhardness test.

Sample	Nitrogen gas flow q_{N2} [sccm]	Vickers microhardness HV [kgf/mm²]
TiS-01	-	413
TiS-04	2.0	1230
TiS-06	3.0	1998
TiS-03	4.0	2027
TiS-05	5.0	2378

The sample TiS-01 developed in the absence of the nitrogen, with a columnar pollycrystaline microstructure, shows a microhardness of 4 GPa. As the reactive gas is introduced in the coating system, the changes in microstructure of the samples leads also to the increasing of the Vickers microhardness. For the fine refined pollycrystaline microstructures the microhardness is in the 12…20 GPa range. In the case of TiS-05 sample, developed with an increase amount of nitrogen the microstructure consists in equiaxial nanocrystalline $Ti_3AlN/TiSi_2$ grains embedded in an amorphous phase and for such a nanocomposite structure the microhardness is high (24 GPa).

Further experimental works are in progress for investigation of structure evolution of the as-deposited coatings and characterization for their high temperature stability.
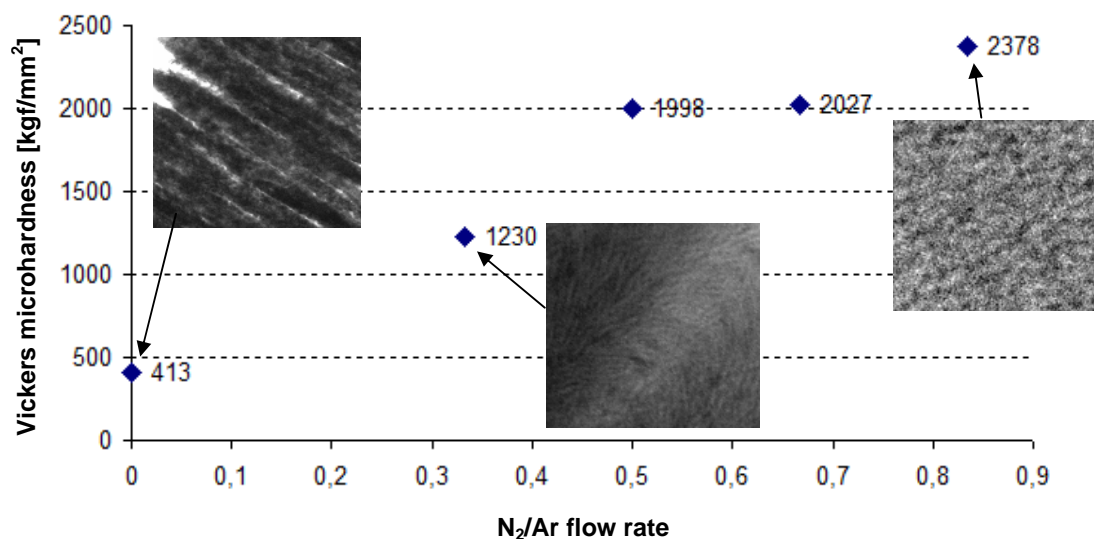

Fig. 6. Vickers microhardness as a function of N_2/Ar gases flow rates; inserts shows the microstructure TEM images of the respective (Ti, Al, Si)N coatings.

4. Conclusions

In the present work it was shown that:

a) Columnar structured polycrystalline AlTiSi thin film coating was developed by non-reactive d.c. magnetron sputtering (performed in pure Ar atmosphere) applied to Al:Ti:Si=50:25:25 alloyed target (where the discharge power 500 W, substrate temperature T_s = 400ºC, bias voltage U_s = –75 V were kept constant);

b) Addition of a small amount of nitrogen to the process gas leads to a crystallite refinement of polycrystalline (Ti, Al, Si)N thin films; increase of nitrogen concentration (q_{N2} = 2 sccm) resulted in fine lamellae growth morphology of nanostructured coatings, consisting of chain-like pearls in a dendrite evolution, clusters of very fine grains in close crystallographic orientation;

c) Further increase in nitrogen amount (q_{N2} = 5 sccm) leads to a nanocomposite structure of (Ti, Al, Si)N coatings consisting of crystalline Ti_3AlN nanograins in 2…3 nm size surrounded by an amorphous Si_xN_y and/or AlN matrix phase;

d) Vickers microhardness of (Ti, Al, Si)N coatings developed with different reactive nitrogen gas flows was found in the 4…24 GPa range; the influence of nitrogen concentration on the increasing of microhardness of the coatings is due to the changes in microstructure, from a columnar structured polycrystalline structure, to a very fine refined one, and than, to a nanocomposite microstructure with nanograins embeded in an amorphous phase.

Acknowledgements

References

[1] J. S. Yoon, H.Y. Lee, J. Han, S.H. Yang, J. Musil, Surface and Coatings Technology **142-144**, 596-602 (2001).

[2] O. Duran-Drouhin, A.E. Santana, A. Karimi, Surface and Coatings Technology **163-164**, 260-266 (2000).

[3] J. Musil, H. Hruby, Thin Solid Films **365**, 104-109 (2000).

[4] E. Ribeiro, A. Malczyk, S. Carvalho, L. Rebouta, J. V. Fernandes, E.Alves, A.S. Miranda, Surface and Coatings Technology **151-152**, 515-520 (2002).

[5] S. Veprek, Thin Solid Films **317**, 449-454 (1998).

[6] M. Parlinska-Wojtan, A. Karimi, T. Cselle, M. Morstein, Surface and Coatings Technology **177-178**, 376 (2004).

[7] M. Parlinska-Wojtan, A. Karimi, O. Coddet, T. Cselle, M. Morstein, Surface and Coatings Technology **188-189**, 344 (2004).

[8] S. Veprek, M.G.J. Veprek-Heijman, P. Karvankova, J. Prochazka, Thin Solid Films **476**, 1 – 29 (2005).

[9] J. Prochazka, P. Karvankova, M.G.J. Veprek-Heijman, S. Veprek, Materials Science and Engineering **384**, 102-116 (2004).

[10] D. Biro, P.B. Barna, L. Szekely, O. Geszti, T. Hattori, A. Devenyi, Nuclear Instruments and Methods in Physics Research A **590**, 99-106 (2008).

[11] J.L. Lábár, Proceedings of the XII EUREM, **III**, 379, (2000).

[12] S. Carvalho, L. Rebouta, E. Ribeiro, F. Vaz, M.F. Dennnot, J. Pacaud, J.P. Riviere, F. Paumier, R. J. Gaboriaud, E. Alves, Surface and Coatings Technology **177-178**, 369 (2004).

[13] S. Carvalho, L. Rebouta, A. Cavaleiro, L.A. Rocha, J. Gomes, E. Alves, Thin Solid Films **398-399**, 391-396 (2001).

[14] F. Vaz, L. Rebouta, P. Goudeau, J. Pacaud, H. Garem, J.P. Riviere, A. Cavaleiro, E. Alves, Surface and Coatings Technology **133-134**, 307-313 (2000).

_____
[*]Corresponding author: strnad@engineering.upm.ro